



FRET- based immunoassay using CdTe and AuNPs for the detection of OmpW antigen of *Vibrio cholerae*



Samira Bagdeli^a, Ali Hossein Rezayan^{a,*}, Ramezan Ali Taheri^b, Mehdi Kamali^b, Morteza Hosseini^a

^a Department of Life Science Engineering, Faculty of New Sciences & Technologies, University of Tehran, Tehran, Iran

^b Nanobiotechnology Research Center, Baqiyatallah University of Medical Sciences, Tehran, Iran

ARTICLE INFO

Keywords:

Förster resonance energy transfer (FRET)
Au nanoparticles (AuNPs)
Quantum dots (QDs)
Outer membrane protein
Vibrio cholerae

ABSTRACT

In the past few decades, nanoscales Förster resonance energy transfer (FRET) based techniques have been used to improve the bioanalysis applications. In this study a new FRET immunosensor based on CdTe was developed for detection of *Vibrio cholerae* outer membrane protein W (OmpW). The assay is based on competitive quantum dot fluorescence quenching by Au nanoparticles (AuNPs). AuNPs with maximum absorption around 517 nm and average size of 14.5 nm was synthesized using the Turkevich method. The Surface of particles was modified with 11-MUA and was conjugated with OmpW via amine coupling method. Formation of Au-OmpW was confirmed by FTIR. Carboxyl functionalized CdTe was conjugated to polyclonal anti-OmpW in the same way. Due to interaction of OmpW with its related antibody, the distance between two particles becomes less than 10 nm and the energy of CdTe transfers to AuNP and cause to decrease of emission intensity. The more the ratio of Au-OmpW, the more quenching of fluorescent emission of CdTe-anti-OmpW via FRET process. By addition of free OmpW, competition between free and conjugated OmpW will cause separation of Au-OmpW from CdTe-anti-OmpW and results in fluorescent recovery. Increase in fluorescence intensity is proportional to the concentration of free OmpW in the analyte solution. The lowest concentration of OmpW that was detected in this study was 2 nM and the linear range of detection was determined to be 2–10 nM. This method is simple, fast and sensitive and also doesn't need any washing step and requires no specific equipment.

1. Introduction

According to the statistics, cholera is an endemic disease in the Indian subcontinent, Russia and sub-Saharan Africa and mostly spread via contaminated water and unsanitary condition. As reported by the World Health Organization (WHO), about 200,000 people are infected with the disease annually [1]. The threat posed by this disease, indicate the necessity of rapid detection of pathogens for control and eradication of the disease [2].

Optical biosensing methods of pathogens are powerful alternatives to conventional analytical techniques for their particularly high specification, sensitivity, small size, and cost effectiveness. They are fast and capable to multiplex detection within a single device and are not prone to electromagnetic interference [3,4]. One of the optical detection methods is Förster resonance energy transfer (FRET) that was described in 1948 by Theodor Förster. FRET is a mechanism describing energy

transfers from a donor in excited energy state to a nearby acceptor chromophore and is revealed by reduction of donor fluorescence emission intensity or increase in acceptor emission intensity. Energy transfer occurs only over short distances than a critical radius known as the Forster radius and is effective in the efficiency of energy transfer. Therefore, FRET is a suitable technique for studying the changes in distance between two sites on a macromolecule or two molecules, such as what happen during protein interactions, enzyme activity, and protein conformational changes [5,6]. Interaction between antibody and antigen can bring donor and acceptor in the distance under critical radius result in energy transfer from donor to acceptor. In comparison to traditional immunoassays such as enzyme-linked immunosorbent assay (ELISA) and lateral flow immunoassay, FRET-based immunoassays have advantages including fast liquid-phase binding kinetics, long-term stability, ratiometric measurement, and homogeneous immunoassay with no washing and separation steps [7].

Abbreviations: OMP, outer membrane proteins; *V. cholerae*, *Vibrio cholerae*; FRET, Förster resonance energy transfer; AuNPs, Au nanoparticle; 11 MUA, 11-mercaptopundecanoic acid; WHO, world health organization; ELISA, enzyme-linked immunosorbent assay; QDs, Quantum Dots; NHS, N-hydroxysuccinimide; EDC, N-(3-Dimethylaminopropyl)-N-ethylcarbodiimide hydrochloride; TMB, 3,3',5,5'-Tetramethylbenzidine; Ni-NTA, Ni-Nitrilotriacetic acid; DLS, Dynamic light scattering; ELS, Electrophoretic light scattering; SAM, self-assembled monolayer; SDS PAGE, sodium dodecylsulphate polyacrylamide gel electrophoresis; FTIR, fourier transform infrared

* Corresponding author.

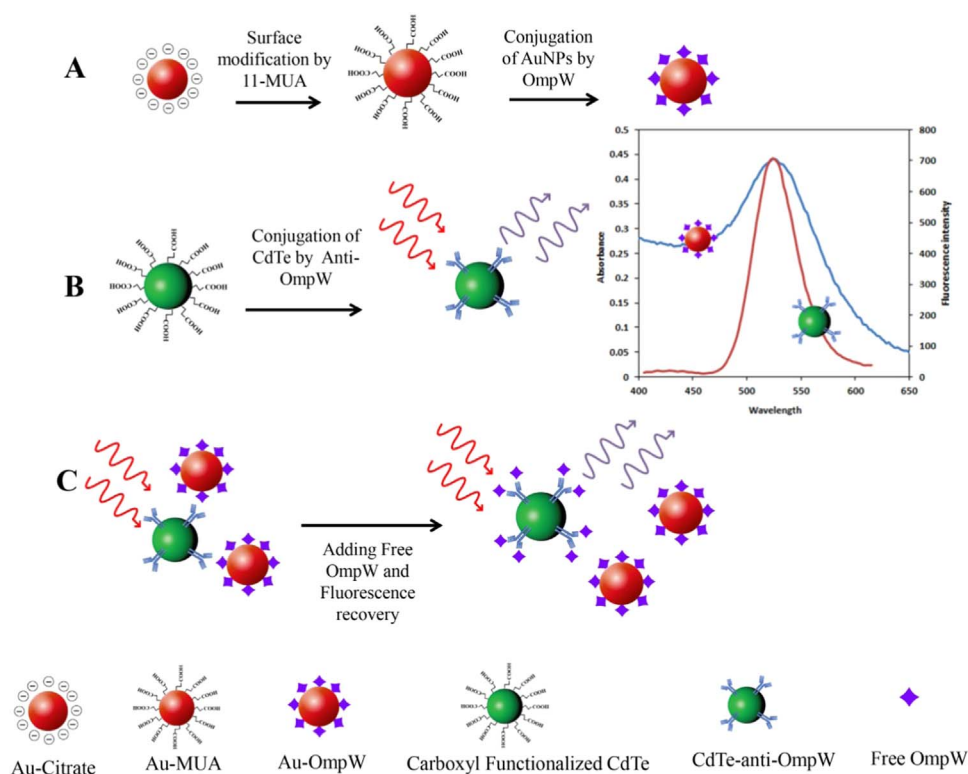
E-mail address: ahrezayan@ut.ac.ir (A.H. Rezayan).

<http://dx.doi.org/10.1016/j.jlumin.2017.08.032>

Received 29 December 2016; Received in revised form 11 August 2017; Accepted 17 August 2017

Available online 18 August 2017

0022-2313/ © 2017 Elsevier B.V. All rights reserved.



Scheme 1. Schematic illustration of (A) preparation of Au-OmpW, (B) anti-OmpW conjugation by CdTe and (C) the competitive homogenous CdTe-FRET immunoassay for detection of OmpW.

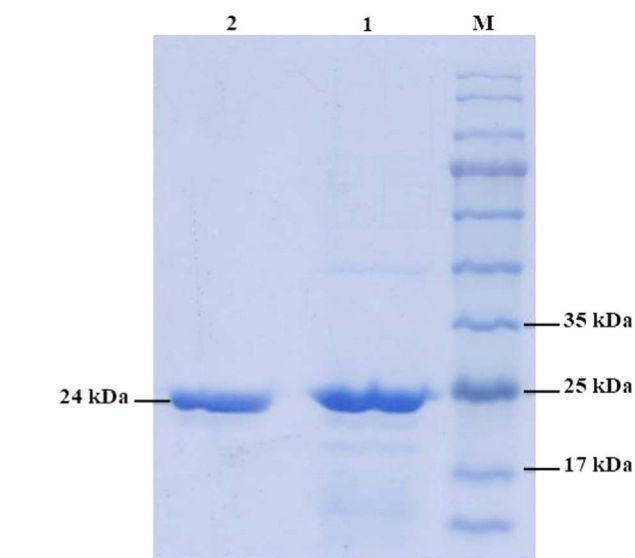


Fig. 1. SDS-PAGE analysis of extracted OmpW (lane 1) and purified OmpW (lane 2) on Ni-NTA column after dialysis.

Most of the FRET-based biological researches have used organic dyes or genetically encoded fluorescent proteins as donor or acceptor fluorophores. These conventional fluorophores have several limitations including low photobleaching threshold and low resistance to chemical and photodegradation [8]. Organic dyes have broad emission spectrum, which means emission spectra of many dyes may overlap to a large area. This limits the application of some dyes for biomolecular labeling in measurements that are performed simultaneously. Also, organic dyes have narrow excitation spectra and need light by specific wavelength for excitation [9]. In contrast, quantum dots (QDs) have particular properties such as high quantum yield, high molar extinction coefficients, broad absorption spectra, narrow and symmetric emission bands (30–50 nm), large effective Stokes shifts, and high resistance to

photobleaching and chemical degradation that make them appropriate alternatives to traditional organic dyes, enzymatic labels and isotopic markers [10–12]. Willard and his colleagues used QD as the energy donor in biological researches for first time in 2001 [13].

Recently, gold nanoparticles have been applied in many bioanalysis because of exhibiting many unique size- and shape-dependent physical and optical properties including scattering, absorption and re-emitting the light which can be revealed by spectroscopic techniques. These particles have high surface to volume ratio and their surface can be modified by functional groups to make individual nanoparticles for biological application. These characteristics are largely depending on their size [14–17]. Gold nanoparticles have large extinction coefficient and broad energy absorption bandwidth in visible range that overlap by emission spectrum of many organic dyes and QDs, therefore, they are excellent FRET-based quencher [18,19].

Based on the aforementioned reasons and as a part of our interest in the synthesis of nanomaterials and investigation of their application in diagnosis and treatment [20–25], in this work, we propose a competitive homogenous immunoassay based on FRET between CdTe and gold nanoparticle for detection of recombinant *Vibrio cholerae* OmpW as a model for potential application in detection of *V. cholerae*. In this method, interaction of OmpW and anti-OmpW will cause to bring CdTe and gold nanoparticle close proximally as FRET donor/acceptor and the fluorescence energy of CdTe would transfer to gold nanoparticle via FRET process and emission would have been quenched. Free OmpWs in sample solution restore emission and it can be measured quantitatively (Scheme 1).

2. Materials and methods

2.1. Materials and instruments

1-ethyl 3-(3-dimethylaminopropyl) carbodiimide hydrochloride (EDC), N-hydroxy-succinimide (NHS) and COOH functionalized CdTe was purchased from Sigma-Aldrich, Sodium citrate and $\text{HAuCl}_4 \cdot 3\text{H}_2\text{O}$ was purchased from Merck. HRP conjugated anti rabbit antibody were

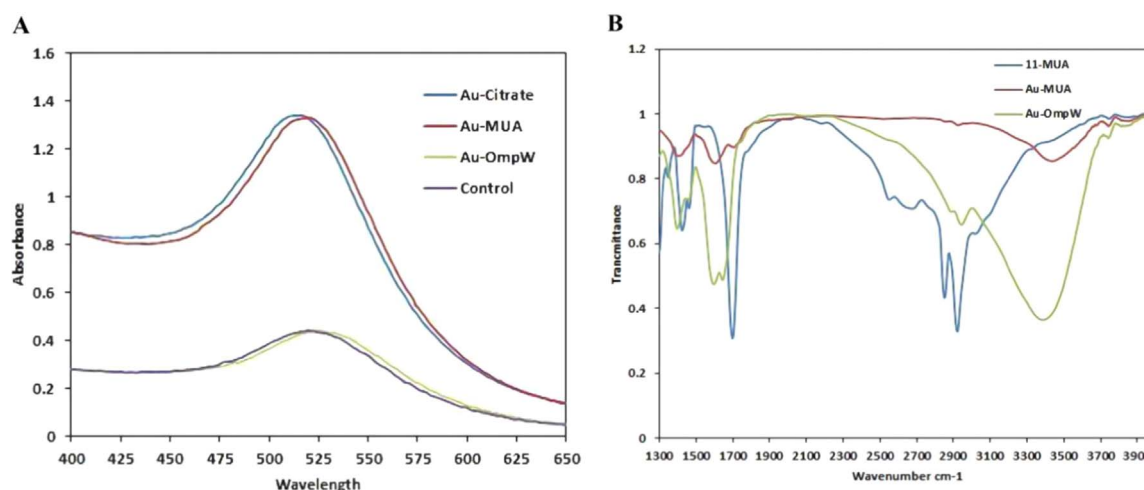


Fig. 2. A: Absorption spectra of Au-citrate, Au-MUA, Au-OmpW and control solution. B: FTIR spectra of 11-MUA, Au-MUA and Au-OmpW. 11-MUA powder and freeze-dried Au-MUA and Au-OmpW were mixed by KBr for pellet preparation.

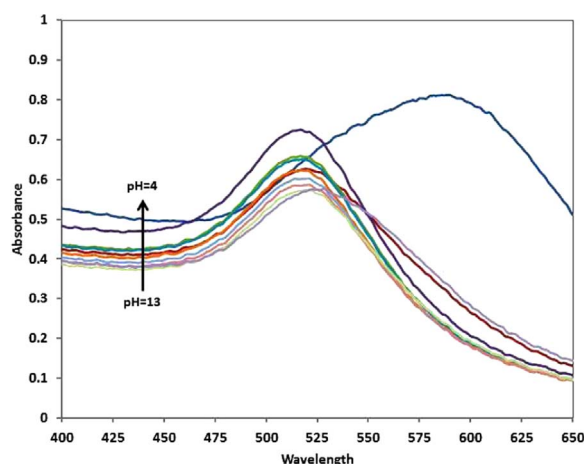


Fig. 3. Absorption spectra of Au-citrate in pH between 4 and 13.

supplied by Razi Biotech (Iran). Tetramethylbenzidine (TMB) was obtained from Monobind Inc and Skim milk was purchased from Roche. The following instruments were used during the study: UV/Vis spectrophotometer (CECIL-CE 7500; Cecil instruments, Cambridge, UK), Nanodrop (Thermo-2000c), Fluorescence spectroscopy (Cary eclipse varian) and Dynamic light scattering (Malvern Zetasizer Nano-ZS).

2.2. OmpW expression and anti-OmpW production

Cloning of OmpW gene fragment had done before in house and the expression of recombinant protein OmpW was performed in *E. coli* BL21

DE3 host cell in optimum conditions followed by extraction with 8 M urea [23–25]. Briefly, the extracted protein was purified by affinity chromatography in denatured conditions using commercially available Ni-Nitrilotriacetic acid (Ni-NTA) columns (Qiagen, Hilden, Germany). Urea was removed by stepwise dialysis against decreasing concentrations of urea (6 M to nil). OmpW band was analyzed via poly acrylamide gel electrophoresis and final protein concentration was determined by Bradford protein assay method. A New Zealand white female rabbit was immunized with purified OmpW according to the following procedure to generate the polyclonal antibody. 200 µg OmpW emulsified by an equal volume of Freund's complete adjuvant was injected to rabbit on day 0. Booster injections carried out with 150 and 100 µg OmpW emulsified in Freund's incomplete adjuvant in day 18 and 32. After 10 days of the last injection, rabbit blood collected and serum was separated from cells by centrifuging. Anti-OmpW isolated from other serum compounds using Montage® antibody purification kit (Millipore, USA), was evaluated by SDS-PAGE with reducing and non-reducing sample buffer and the final concentration of antibody was determined by Bradford protein assay

2.3. AuNPs synthesis and surface modification by 11-MUA

All glassware used in the following procedure was thoroughly cleaned in aqua regia ($\text{HNO}_3\text{--HCl} = 1:3, \text{v/v}$), rinsed in distilled water, and then oven-dried prior to use, to avoid unwanted nucleation during the synthesis, as well as aggregation of gold colloid solutions. The AuNPs were prepared by the citrate reduction method according to the published protocol [26]. Briefly, 10 ml of 0.01% HAuCl_4 was brought to a boil with vigorous stirring. Then 300 µl of 1% sodium citrate was rapidly added to this solution. The mixed solution was stirred for

Table 1

Maximum absorbance of synthesized gold nanoparticle in pH between 4 and 13.

Wave length	A in pH = 4	A in pH = 5	A in pH = 6	A in pH = 7	A in pH = 8	A in pH = 9	A in pH = 10	A in pH = 11	A in pH = 12	A in pH = 13
516	0.638	0.623	0.658	0.724	0.649	0.621	0.6	0.584	0.571	0.563
517	0.641	0.624	0.659	0.725	0.65	0.623	0.601	0.584	0.571	0.566
518	0.646	0.625	0.657	0.723	0.65	0.622	0.601	0.585	0.572	0.569
519	0.65	0.626	0.656	0.72	0.649	0.621	0.601	0.586	0.572	0.569
520	0.654	0.626	0.656	0.719	0.649	0.622	0.602	0.586	0.573	0.571
521	0.657	0.625	0.655	0.72	0.647	0.621	0.602	0.587	0.574	0.573
522	0.66	0.624	0.652	0.717	0.643	0.617	0.6	0.585	0.573	0.575
523	0.665	0.622	0.647	0.712	0.639	0.612	0.595	0.581	0.57	0.575
524	0.67	0.62	0.643	0.709	0.635	0.608	0.592	0.577	0.566	0.574

^a A: absorbance.

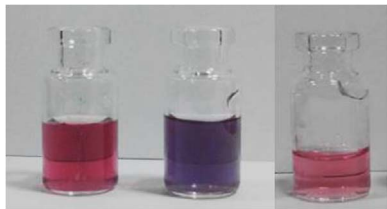


Fig. 4. Salt tolerance test. Left to right: control (Au-MUA, no NaCl), Au-MUA (1% NaCl) and Au-OmpW (5% NaCl).

10 min then removed from the heating mantle and stirring continued for another 5 min in ice for cooling. Prepared AuNPs solution characterized by UV/Vis spectroscopy, Dynamic Light Scattering (DLS) and Electrophoretic light scattering (ELS).

11-mercaptoundecanoic acid (11-MUA) is an alkanethiol that can

bind to gold nanoparticles through its thiol head group as strong as a covalent bond and form self-assembled monolayer (SAM) [27]. AuNP synthesis solution pH was adjusted to 9 by 100 μ l of 0.5 M NaOH (synthesis AuNPs had the highest colloid stability in pH 9) and 40 μ l of 1 mM 11-MUA (ethanol solvent) was added to 10 ml of this solution. The gold colloid solution was stirred overnight at 4 $^{\circ}$ C. The nanoparticles were then centrifuged at 14,000 rpm for 30 min and the supernatant was replaced with pH adjuster water (pH 9) [28].

2.4. OmpW conjugation to AuNPs

11-MUA functionalized AuNPs were covalently coupled with OmpW using EDC/NHS protocol. Different reaction conditions were tested and the result was examined by UV/Vis spectroscopy and salt tolerance test by 1–5% NaCl solution. The following is the optimal protocol developed in the course of this study. Firstly, 2 ml of functionalized AuNPs was

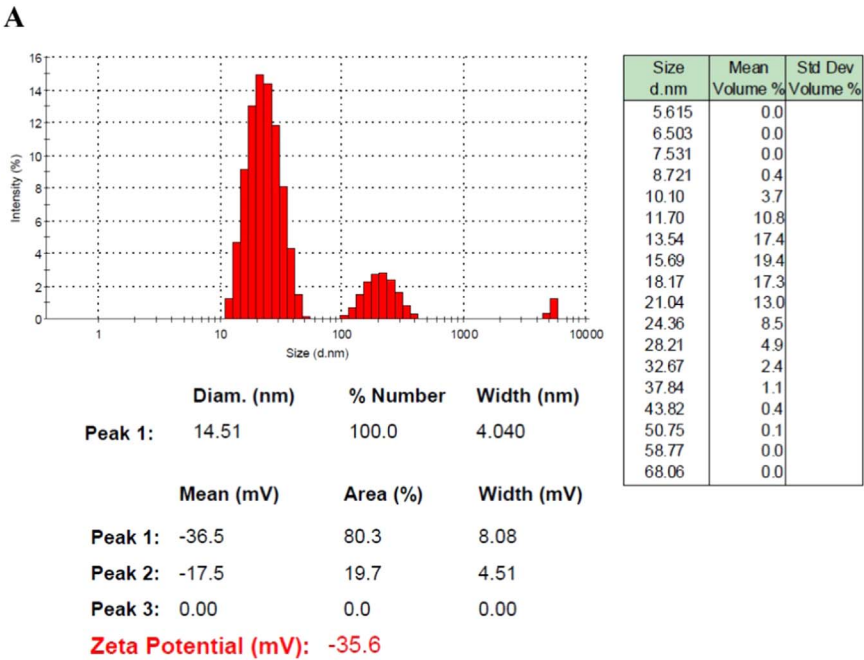
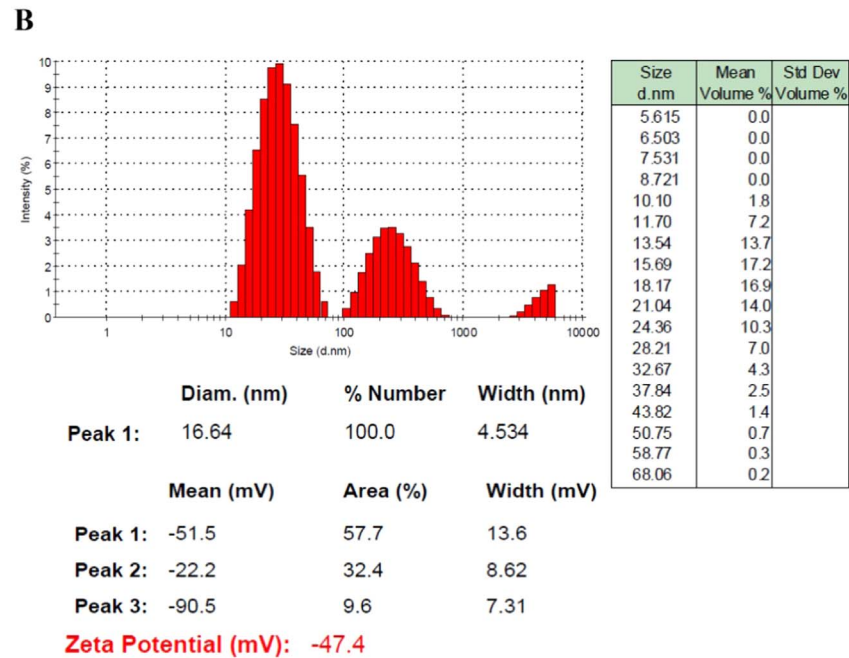


Fig. 5. Size and zeta potential analysis of synthesized (A) and surface modified gold nanoparticle (B).



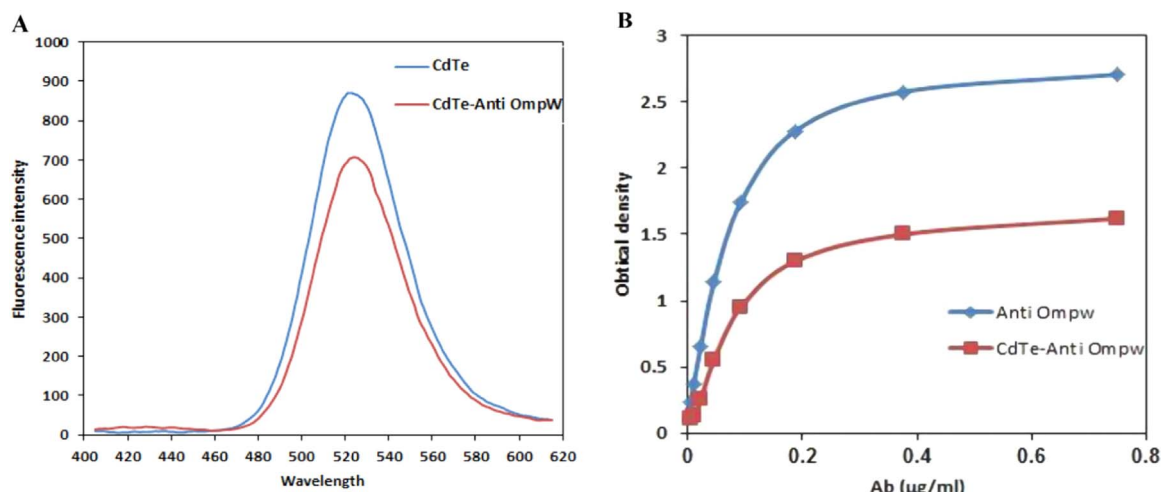


Fig. 6. A: Carboxyl functionalized CdTe fluorescence intensity before and after binding anti-OmpW. B: Indirect ELISA by free and CdTe labeled anti-OmpW in the same concentration.

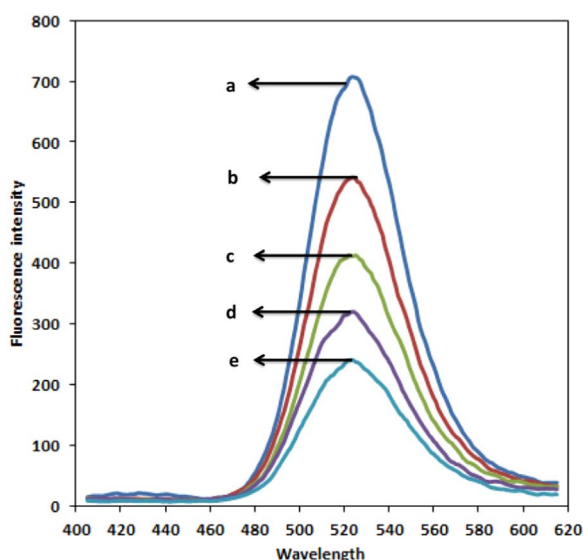


Fig. 7. Fluorescence intensity of 200 µl of CdTe-anti-OmpW (a) after mixing by 100 µl of PBS: Au-OmpW with 1:0 (b), 1:1(c), 1:3(d) and 0:1(e) ratio.

mixed by 2 ml of 1.2 mM NHS and 2.8 mM EDC in PBS buffer (pH 7) with stirring. After few minutes, 2 ml of 200 nM OmpW solution was added to the mixture and incubated for 2 h in room temperature. Unbound OmpWs and other small compounds were removed by centrifuging at 14,000 rpm for 30 min. Formation of Au-OmpW was confirmed by FTIR. In control sample, AuNPs was mixed by EDC/NHS in PBS in the same way but OmpW was not added to the solution.

2.5. Anti-OmpW conjugation to CdTe

Bioconjugation of carboxyl functionalized CdTe (Sigma-Aldrich) with anti-OmpW antibody was carried out according to the following protocol [29–31]. Briefly, 50 µl of 0.5 mM CdTe (buffer PBS, pH 7.4) was mixed with 500 µl of 0.05 M EDC and 500 µl of 5 mM NHS and 1.096 ml of 0.89 µg/ml anti-OmpW and the solution volume was reached to 25 ml by PBS. The solution was incubated in the dark at room temperature for 2 h and then centrifuged for 30 min at 8000 rpm to separate agglomerated particles (if any).

2.6. Immunocomplex formation

Bioconjugate of CdTe-anti OmpW was mixed by series of different

dilutions of prepared Au-OmpW. All mixtures were incubated for 30 min at room temperature. The immunocomplex formation was measured using Cary Eclipse fluorescence spectrophotometer with excitation at 320 nm.

2.7. Competitive Immunoassay

In order to confirm the formation of CdTe-anti OmpW/ Au-OmpW immunocomplex and competitive measurement of free OmpW in sample, serial dilutions of 2–100 nM OmpW was added to immunocomplex solution. At first, according to the aforementioned step, 100 µl Au-OmpW was mixed to 200 µl CdTe-anti OmpW solution and incubated at room temperature for 30 min. After that free OmpWs were added to immunocomplex solution and incubated for another 30 min at room temperature. The competitive immunoassay was measured using Cary Eclipse fluorescence spectrophotometer.

3. Results and discussion

3.1. Production and purification of OmpW antigen

Expression of OmpW in the bacteria caused the formation of inclusion body that revealed in SDS analysis of bacterial lysate as a dominant band in approximately 25 kDa (Fig. 1).

3.2. Characterization of AuNPs after synthesis, surface modification and bioconjugation

UV/Vis spectroscopy of synthesized AuNPs (average size 14.5 nm Fig. 5) determined that these particles have maximum absorption at 517 nm. The surface of the particles is covered by citrate and electrostatic repulsion of citrate carboxylic groups gives rise to the stability of particles. Fig. 2A shows absorption spectra of Au-citrate, Au-MUA, Au-OmpW and control solution. Increasing in the pH of Au-citrate colloid causes to increase in ionization of citrate carboxylic group and subsequently increase in electrostatic repulsion and particle stability. Absorption spectra (Fig. 3) and maximum absorption wavelength (Table 1) of Au-citrate colloid in pH between 4 and 13 shows that synthesized Au-citrate particle had the most stability in pH = 9 (Fig. 4). Maximum absorption peak of AuNPs are red shifted to 519 nm after surface modification by 11-MUA and 525 nm after conjugation by OmpW, while the absorption peak width has not changed and shows particles remain dispersed. Also, there is no change in absorption peak of control solution that means EDC/NHS have no effect on the absorption of light by nanoparticles. In addition, zeta potential analysis of

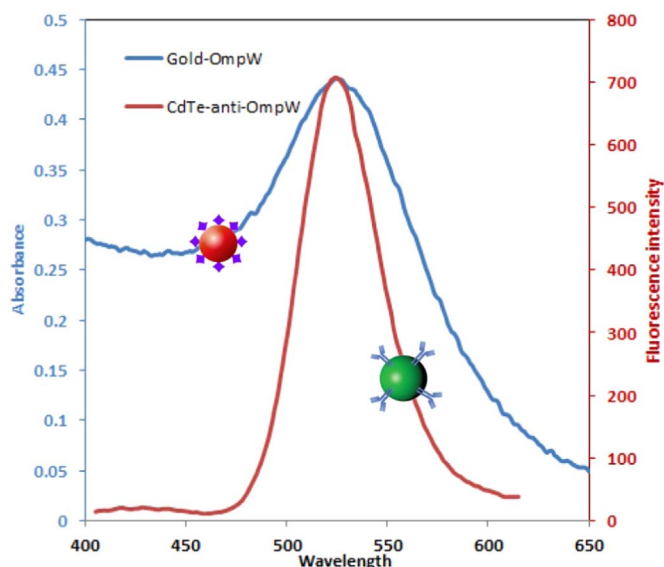


Fig. 8. Overlap between the emission spectrum of CdTe-anti-OmpW and absorption spectrum of synthesized Au-OmpW nanoparticle.

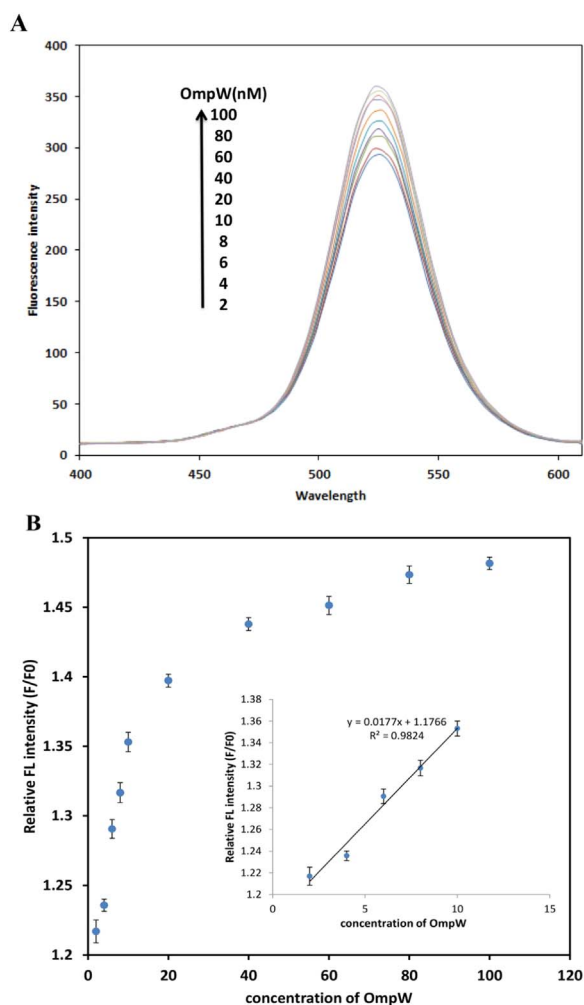


Fig. 9. (A) Fluorescence spectra of CdTe-anti-OmpW in the presence of Au-OmpW with varying concentration of free OmpW. (B) Calibration curve of OmpW and linear plot of relative FL intensity (F/F₀). F₀ and F denote fluorescence intensity in CdTe-antiOmpW/Au-OmpW solution before and after adding OmpW serial dilutions respectively.

Au-citrate and Au-MUA shows change in surface charge of particle (Fig. 5).

FTIR spectra of 11-MUA, Au-MUA and Au-OmpW are shown in Fig. 2B. Two peaks in free 11-MUA spectra in 2675 cm⁻¹ and 2549 cm⁻¹ are related to S-H stretching mode and have been disappeared in Au-MUA spectra and shows formation of 11-MUA self-assembled monolayer on gold surface via Au-S bonding. In Au-OmpW spectrum, the peak in 1640 cm⁻¹ are related to amide bond.

Also, the salt tolerance test results showed that Au-MUA particles aggregated in the presence of 1% NaCl but Au-OmpW particles remained dispersed even after adding of 5% NaCl and their absorption didn't change. It means that particle surfaces are completely covered by OmpW (Fig. 4).

3.3. Conjugation of antibody to CdTe

As shown in Fig. 6A, CdTe fluorescent intensity has been reduced after conjugation to anti-OmpW because of coupling agents like EDC/NHS and covalent bond between carboxyl group on CdTe surface and antibody amine group. Also, the emission spectrum width doesn't change because CdTe particles are not connected to each other through the process of antibody binding and thus remain stable.

In order to investigate the anti-OmpW antibody activity after conjugation to CdTe, indirect ELISA for free antibody and CdTe-anti-OmpW with the same amount of OmpW were performed. Results are shown in Fig. 6B. As can be seen in Fig. 6B, after conjugating of antibody to CdTe, the interaction between antibody and antigen decreased dramatically. This is maybe because of random orientation of antibody attached to CdTe. It is interesting to note that polyclonal antibodies are heterogeneous and recognize a host of antigenic epitopes, therefore, their use in diagnostic systems that requires antibody labeling or antigen stabilization has less impact on overall function.

3.4. Immunocomplex formation

High affinity interaction between OmpW and anti-OmpW ($K_D = 2.4 \pm 0.07 \times 10^{-9}$ M) was reported before [23–25]. In this work, study of changes in fluorescence spectra of CdTe-anti-OmpW solution after mixing by gradually increasing quantity of Au-OmpW, showed decrease in fluorescence intensity in 535 nm (Fig. 7). This indicated that after mixing of CdTe-anti-OmpW and Au-OmpW solution, the distance between gold nanoparticles and CdTe are reduced because of the specific interaction of OmpW and anti-OmpW and the excited energy of CdTe was transferred to the gold nanoparticle through FRET process, result in decrease in CdTe-anti-OmpW emission. Different ratios of Au-OmpW was checked and the results showed that the Au-OmpW binding to the CdTe-anti-OmpW reduce the emission of solution and the more Au-OmpW in solution, the more quenching of fluorescent emission via FRET process.

The overlap between donor emission spectrum and acceptor absorption spectrum is one of effective factors on FRET efficiency (E_{FRET}). The FRET efficiency is defined as the number of quanta transferred to the acceptor divided by the number of quanta absorbed by the donor. Fig. 8 shows the overlap between the emission spectrum of CdTe and absorption spectrum of synthesized gold nanoparticle. According to the suitable overlap between CdTe emission and synthesized gold nanoparticles, it is assumed that the resonance energy transfer was done effectively. E_{FRET} between the CdTe-anti-OmpW and Au-OmpW was calculated 55.4%. using the following equation:

$$E_F = 1 - (F'D/FD)$$

where, F'D is emission intensity of donor in the presence of acceptor and FD is emission intensity in the absence of acceptor.

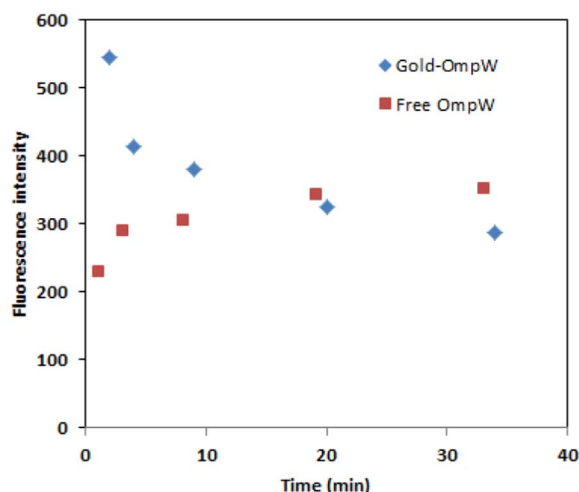


Fig. 10. Fluorescence intensity recorded at different time of immunocomplex formation.

3.5. Measurement of free OmpW in sample

As shown in Fig. 9A, changes in fluorescence intensity of immunocomplex solution after adding serial dilution of free OmpW show that free OmpW compete with Au-OmpW for antibody binding site and replace with them in the immunocomplex and thereby inhibit FRET process. This events led to increase the distance between CdTe-anti-OmpW (energy donor) and Au-OmpW (energy acceptor) become more than the critical radius and the resonance energy transfer doesn't occur, so that the fluorescence intensity would be recovered (Fig. 9A). Increasing the amount of free OmpW (2–100 nM) results in increase in fluorescence recovery in solution until the solution response reach to equilibrium. The lowest amount of free OmpW we have detected in this study was 2 nM (Fig. 6B) and the linear range of detection was between 2 and 10 nM (Fig. 6B inset).

Dynamics of immune complex formation after the addition of Au-OmpW and free OmpW to CdTe-anti-OmpW solution were measured at different times. As shown in Fig. 10, in both solutions formation of immune complexes occurred more quickly in the first few minutes and after incubation for 30 min interactions performed at constant speed.

For comparing the detection limit of our work with the others it is interesting to note that FRET-based method for detection of *salmonella* and *listeria* surface antigens was reported by Ko and Grant [32], in which the detection limit was 2 µg/ml and also in another research the detection limit for dengue viral antigens was 5 µg/ml based on Quartz Crystal Microbalance (QCM) [33], while in the present study the lowest amount for free OmpW detection was 2 nM (Fig. 6B).

4. Conclusion

In this paper, a novel FRET biosensor was developed comprised of antibody conjugated CdTe and OmpW conjugated AuNP for quantitative detection of free OmpW in sample. In comparison with heterogeneous methods such as ELISA, this method doesn't need washing steps, so antigen and antibody don't detach during washing step. Also, FRET requires no specific equipment beyond fluorescence spectroscopy and gives a strong signal in the lowest time and has high sensitivity to small amount of analyte. As the current study was based on competitive quantum dot fluorescence quenching by Au nanoparticles, the protocol could be used in detection of whole *V. cholerae* bacterial cells by adding bacterial suspensions instead of free OmpW antigen and quantify the test by standard dilutions of *V. cholerae*. Moreover, the present method can be expand to quantitative analysis of various important compounds like toxins, bacterial virulence factors and other environmental and clinical targets, and it has great potential in designing assay system for

detection of viable but non culturable (VBNC) bacterial species that don't have ability to grow on culture medium.

Acknowledgments

This paper has been extracted from MSc thesis. The authors would like to acknowledge the financial support of Baqiyatallah University of Medical Sciences (Grant no. 91-1127).

References

- [1] P. Tallury, A. Malhotra, L.M. Byrne, S. Santra, Nanobioimaging and sensing of infectious diseases, *Adv. Drug Deliv. Rev.* 62 (2010) 424–437.
- [2] J. Reidl, K.E. Klose, *Vibrio cholerae* and cholera: out of the water and into the host, *FEMS Microbiol. Rev.* 26 (2002) 125–139.
- [3] D. Dey, T. Goswami, Optical biosensors: a revolution towards quantum nanoscale electronics device fabrication, *BioMed. Res. Int.* 2011 (2011).
- [4] X. Fan, I.M. White, S.I. Shopova, H. Zhu, J.D. Suter, Y. Sun, Sensitive optical biosensors for unlabeled targets: a review, *Anal. Chim. Acta* 620 (2008) 8–26.
- [5] N.-T. Chen, S.-H. Cheng, C.-P. Liu, J.S. Souris, C.-T. Chen, C.-Y. Mou, et al., Recent advances in nanoparticle-based Förster resonance energy transfer for biosensing, molecular imaging and drug release profiling, *Int. J. Mol. Sci.* 13 (2012) 16598–16623.
- [6] L. Shi, C. Jing, Z. Gu, Y.-T. Long, Brightening gold nanoparticles: new sensing approach based on plasmon resonance energy transfer, *Sci. Rep.* 5 (2015) 10142.
- [7] W. Xu, Y. Xiong, W. Lai, Y. Xu, C. Li, M. Xie, A homogeneous immunosensor for AFB1 detection based on FRET between different-sized quantum dots, *Biosens. Bioelectron.* 56 (2014) 144–150.
- [8] A.R. Clapp, I.L. Medintz, H. Mattoussi, Förster resonance energy transfer investigations using quantum-dot Fluorophores, *ChemPhysChem* 7 (2006) 47–57.
- [9] T. Jamieson, R. Bakhshi, D. Petrova, R. Pocock, M. Imani, A.M. Seifalian, Biological applications of quantum dots, *Biomaterials* 28 (2007) 4717–4732.
- [10] F.A. Esteve-Turrillas, A. Abad-Fuentes, Applications of quantum dots as probes in immunosensing of small-sized analytes, *Biosens. Bioelectron.* 41 (2013) 12–29.
- [11] K.E. Sapsford, L. Berti, I.L. Medintz, Materials for fluorescence resonance energy transfer analysis: beyond traditional donor–acceptor combinations, *Angew. Chem. Int. Ed.* 45 (2006) 4562–4589.
- [12] D. Singh, S. Pandey, R. Manohar, S. Kumar, G. Pujar, S. Inamdar, Time-resolved fluorescence and absence of Förster resonance energy transfer in ferroelectric liquid crystal-quantum dots composites, *J. Lumin.* 190 (2017) 161–170.
- [13] D.M. Willard, L.L. Carillo, J. Jung, A. Van Orden, CdSe-ZnS quantum dots as resonance energy transfer donors in a model protein-protein binding assay, *Nano Lett.* 1 (2001) 469–474.
- [14] E. Chatterjee, Detection Techniques for Biomolecules Using Semi-conductor Nanocrystals and Magnetic Beads as Labels, 2011.
- [15] X. Huang, P.K. Jain, I.H. El-Sayed, M.A. El-Sayed, Gold nanoparticles: interesting optical properties and recent applications in cancer diagnostics and therapy, *Nanomedicine* (2007).
- [16] X. Liu, M. Atwater, J. Wang, Q. Huo, Extinction coefficient of gold nanoparticles with different sizes and different capping ligands, *Colloids Surf. B Biointerfaces* 58 (2007) 3–7.
- [17] D.A. Giljohann, D.S. Seferos, W.L. Daniel, M.D. Massich, P.C. Patel, C.A. Mirkin, Gold nanoparticles for biology and medicine, *Angew. Chem. Int. Ed.* 49 (2010) 3280–3294.
- [18] K. Jiang, A.O. Pinchuk, Chapter two-noble Metal nanomaterials: synthetic routes, fundamental properties, and promising applications, *Solid State Phys.* 66 (2015) 131–211.
- [19] K. Saha, S.S. Agasti, C. Kim, X. Li, V.M. Rotello, Gold nanoparticles in chemical and biological sensing, *Chem. Rev.* 112 (2012) 2739–2779.
- [20] M. Hosseini, A. Akbari, M.R. Ganjali, M. Dadmehr, A.H. Rezayan, A novel label-free microRNA-155 detection on the basis of fluorescent silver nanoclusters, *J. Fluoresc.* 25 (2015) 925–929.
- [21] A. Nikfarjam, A.H. Rezayan, G. Mohammadkhani, J. Mohammadnejad, Label-free detection of digoxin using localized surface plasmon resonance-based nanobiosensor, *Plasmonics* (2016) 1–8.
- [22] A.H. Rezayan, M. Mousavi, S. Kheirjou, G. Amoabediny, M.S. Ardestani, J. Mohammadnejad, Monodisperse magnetite (Fe₃O₄) nanoparticles modified with water soluble polymers for the diagnosis of breast cancer by MRI method, *J. Magn. Magn. Mater.* 420 (2016) 210–217.
- [23] R.A. Taheri, A.H. Rezayan, F. Rahimi, J. Mohammadnejad, M. Kamali, Comparison of antibody immobilization strategies in detection of *Vibrio cholerae* by surface plasmon resonance, *Biointerphases* 11 (2016) 041006.
- [24] R.A. Taheri, A.H. Rezayan, F. Rahimi, J. Mohammadnejad, M. Kamali, Development of an immunosensor using oriented immobilized anti-OmpW for sensitive detection of *Vibrio cholerae* by surface plasmon resonance, *Biosens. Bioelectron.* 86 (2016) 484–488.
- [25] R.A. Taheri, A.H. Rezayan, F. Rahimi, J. Mohammadnejad, M. Kamali, Evaluating the potential of an antibody against recombinant OmpW antigen in detection of *Vibrio cholerae* by surface plasmon resonance (SPR) biosensor, *Plasmonics* (2016) 1–12.
- [26] K.C. Grabar, R.G. Freeman, M.B. Hommer, M.J. Natan, Preparation and characterization of Au colloid monolayers, *Anal. Chem.* 67 (1995) 735–743.

- [27] S.-Y. Lin, Y.-T. Tsai, C.-C. Chen, C.-M. Lin, C.-h. Chen, Two-step functionalization of neutral and positively charged thiols onto citrate-stabilized Au nanoparticles, *J. Phys. Chem. B* 108 (2004) 2134–2139.
- [28] M.R. Ivanov, Covalently Functionalized Gold Nanoparticles: Synthesis, Characterization, and Integration into Capillary Electrophoresis, (2011).
- [29] Y. Li, Q. Ma, X. Wang, X. Su, Fluorescence resonance energy transfer between two quantum dots with immunocomplexes of antigen and antibody as a bridge, *Luminescence* 22 (2007) 60–66.
- [30] S. Wang, N. Mamedova, N.A. Kotov, W. Chen, J. Studer, Antigen/antibody immunocomplex from CdTe nanoparticle bioconjugates, *Nano Lett.* 2 (2002) 817–822.
- [31] X. Zhu, L. Chen, P. Shen, J. Jia, D. Zhang, L. Yang, High sensitive detection of Cry1Ab protein using a quantum dot-based fluorescence-linked immunosorbent assay, *J. Agric. Food Chem.* 59 (2011) 2184–2189.
- [32] S. Ko, S.A. Grant, Development of a novel FRET method for detection of *Listeria* or *Salmonella*, *Sens. Actuators B: Chem.* 96 (2003) 372–378.
- [33] C.-C. Su, T.-Z. Wu, L.-K. Chen, H.-H. Yang, D.-F. Tai, Development of immunochips for the detection of dengue viral antigens, *Anal. Chim. Acta* 479 (2003) 117–123.